# Adsorption of Sodium Poly(styrenesulfonate) to the Air Surface of Water by Neutron and X-ray Reflectivity and Surface Tension Measurements: Polymer Concentration Dependence

**H. Yim, M. S. Kent,* A. Matheson, and M. J. Stevens**

*Sandia National Laboratories, Albuquerque, New Mexico 87185-1411*

**R. Ivkov and S. Satija**

*National Institute of Standards and Technology, Gaithersburg, Maryland*

**J. Majewski and G. S. Smith**

*LANSCE, Los Alamos National Laboratories, Los Alamos, New Mexico*

*Received January 10, 2002*

ABSTRACT: The adsorption of the strong polyelectrolyte sodium poly(styrenesulfonate) (NaPSS) to the air surface of water was investigated as a function of polymer concentration from the dilute regime to the beginning of the semidilute regime. Detailed segment profiles of the deuterated polymer were determined by neutron reflection (NR). Data were obtained for 0.67 and 2.50 M KCl. For two samples differing widely in molecular weight (1150 and 56.1 kg/mol), we find that with increasing polymer concentration the adsorbed amount first increases, reaches a maximum, and then decreases strongly. The PSS concentration at which the maximum is reached is dependent on both the molecular weight and the salt concentration in a manner that correlates with the chain overlap concentration. Regarding the segment profiles, at low polymer concentration the profiles are composed of a thin layer of high concentration at the air surface (trains), followed by a distinct second layer of much lower segment concentration that extends to larger depths into the liquid (loops and tails). Complementary X-ray reflection (XR) revealed a localization of ions about 10 Å below the surface for dilute PSS concentration. This layer becomes more diffuse at higher PSS concentration, in conjunction with the decrease in PSS adsorbed amount measured by NR. This surprising behavior of the adsorbed amount with polymer concentration is not explained by current SCF theory treating the adsorption of strong polyelectrolytes to neutral surfaces. We discuss a few possible explanations for this desorption transition. Finally, we observe that the surface tension decreases monotonically with increasing concentration of PSS in bulk solution but is not correlated with the adsorbed amount of PSS at the surface.

## Introduction

The adsorption of polyelectrolytes onto surfaces is important in many technologies. Polyelectrolyte adsorption onto colloid surfaces plays a central role in the stabilization of emulsions in food, photographic, and pharmaceutical industries.[1,2] The adsorption of biological polyelectrolytes is a key step in many biochemical processes. Understanding such processes is also important for controlling fouling in biotechnological operations and for controlling biocompatibility in biomedical applications.[3] From a fundamental point of view, it is important to investigate how the conformation of a polyelectrolyte is changed near an interface and the factors which control the conformation, the adsorbed amount, and the distribution of counterions.[4]

The present work focuses on the variation in the adsorption of strong polyelectrolytes with bulk polyelectrolyte concentration. We are concerned with variations in the adsorbed amount and the conformations of the adsorbed chains. In bulk solution, experimental studies of polyelectrolyte concentration effects have focused on variations in correlation lengths by neutron[5−9] and light[10−13] scattering, along with rheological properties.[9,14,15] Recently, Takahashi et al. reported radii of gyration for sodium poly(styrenesulfonate) (NaPSS) in pure water over a range of NaPSS concentration in the semidilute and concentrated regimes by neutron scattering.[16] Polyelectrolyte chain conformations have not been directly studied in the dilute regime due to the limited sensitivity of the experimental techniques. Theoretical understanding of polyelectrolyte systems has been hampered due to the complication of the long-range nature of the Coulomb interaction, which cannot be handled presently beyond the linear Debye−Hückel approximation, which surely breaks down for strong polyelectrolytes. In particular, for salt-free solutions the regime in which neither Coulomb interactions nor entropy dominates cannot be accurately treated at present. In this case, the counterions are neither entirely condensed on the chains nor entirely free but are distributed between the two states. Recently, Stevens and Kremer[17] reported molecular dynamics simulations of linear polyelectrolytes in solution. They covered a range of concentrations from dilute to semidilute. In contrast to the predicted dilute limit of rodlike chains, they found that the polyelectrolyte chains have significant bending even at very low polymer concentrations. Furthermore, the chains begin to contract at concentrations roughly an order of magnitude lower than the chain overlap concentration. This is due to the overlap of the counterion clouds. In the presence of high salt concentration, the counterions exchange rapidly with free ions, and the concept of a counterion cloud is no longer valid.

Several experimental studies have been reported on the adsorption of polyelectrolytes to interfaces as a

10.1021/ma0200468 CCC: $22.00 
Published on Web 11/14/2002

function of polyelectrolyte concentration.[18−22] Papenhuijzen et al. studied the adsorption of PSS onto poly(oxymethylene) single crystals.[18] They found that the adsorbed amount increased with PSS concentration and molecular weight as well as with ionic strength. However, the PSS concentration range they studied was much lower than in the present study. Detailed concentration profiles near the substrate were not reported. Okubo,[19] Okubo and Kobayashi,[20] Gaminati and Gabrielli,[21] and Theodoly et al.[22] used surface tension measurements to study the adsorption of various polyelectrolytes to the air surface of water as a function of polyelectrolyte concentration. They examined polyelectrolyte concentrations ranging from dilute to semidilute. Attempts were made to infer adsorbed amounts and polymer conformations indirectly from decreases in surface tension.

We have chosen the air surface of aqueous solutions as a model interface for studying the adsorption of polyelectrolytes. This provides a straightforward and reproducible interface which is easily probed with X-rays and neutrons and also allows the free energy to be probed through surface tension measurements. In previous work,[23] we examined the adsorption of the strong polyelectrolyte poly(*d*-styrenesulfonate) (d-PSS) from dilute solution (0.001 g/mL) to the air surface of water as a function of molecular weight and salt concentration by neutron reflection (NR). In the limit of low salt concentration, the profile tends toward a conformation consisting of mainly a thin dense surface layer, i.e., mostly trains with few segments extending into the subphase. At higher salt concentration, the data indicated a bilayer profile with a thin layer (∼20 Å) of very high segment concentration at the air surface and a distinct second layer of much lower segment concentration which extends much further into the subphase. The adsorbed amount increased with salt concentration, with a stronger dependence for higher molecular weight chains. While the trends of adsorbed amount and layer thickness were consistent with the predictions of numerical self-consistent-field (SCF) theory for adsorption at a neutral surface, the measured bilayer profiles contrasted with the smoothly decaying theoretical profiles.

In the present work we report the adsorption of d-PSS to the air surface of water as a function of d-PSS concentration for two widely different molecular weights. For the first time we combine direct measurements of the adsorbed amount of polyelectrolyte (by neutron reflection), the ion distribution (by X-ray reflection), and the free energy (by surface tension measurements). We study d-PSS concentrations ranging from the dilute regime to the beginning of the semidilute regime. While many previous studies have drawn inferences about the adsorbed amount from variations in the surface tension,[19−22] we find that there is no correlation between adsorbed amount and the surface tension. Another important finding is that a maximum in adsorbed amount occurs with increasing PSS concentration. This surprising result is the main topic of this report.

## Experimental Section

**Materials.** Two deuterated sodium poly(styrenesulfonate) samples were used. d-PSS56, with molecular weight of 56 100 g/mol (excluding $Na^+$ counterion) and $M_w/M_n = 1.06$, was obtained from Polymer Source and used as received. For the second sample, dPSS1150, d-PS of molecular weight 708 000 g/mol and $M_w/M_n = 1.03$ was obtained from Pressure Chemical Co. and sulfonated using the method of Vink.[24] A solution was prepared by dissolving 1 g of d-PS in 100 mL of cyclohexane. This solution was added dropwise to a solution of 6 g of $P_2O_5$ in 27 mL of $H_2SO_4$ at 50 °C. The solution was stirred for 60 min and then allowed to stand for an additional 60 min without stirring. The solution was cooled in an ice bath, and then 17 g of frozen $H_2O$ were added. In this process a yellowish-white sticky mass was obtained. The product was washed with distilled water several times, dissolved in 300 mL of water, and then purified by dialysis against deionized water for 1 week. Finally, the product was neutralized and recovered as the sodium salt by freeze-drying. The sulfonization level of both samples was roughly 90% by NMR.

**Methods.** For the NR experiments, the solutions were prepared by first dissolving the d-PSS in an $H_2O/D_2O$ mixture (v/v 0.843/0.157) at the desired concentration, followed by addition of KCl. After mixing, the solutions were allowed to equilibrate for at least 6 h prior to use. The composition of the aqueous solvent was chosen to optimize the neutron scattering contrast while maintaining a measurable critical edge for total reflection for normalization. The neutron scattering length density (SLD) of the pure subphase was $0.530 \times 10^{-6}$ Å$^{-2}$, which corresponds to a critical edge for total reflection of neutrons at $q_c = 0.0052$ Å$^{-1}$, where $q = 4\pi\sin\theta/\lambda$. Fresh solution was prepared for each reflectivity experiment. The solution was contained in a Teflon trough at room temperature. Roughly 20 min passed between the time the solution was poured into the trough and the beginning of data collection. The runs were repeated at ∼4 h intervals until successive runs gave identical (within the error bars) reflectivity curves. The neutron reflectivity (NR) measurements were performed on the NG7 reflectometer at NIST using a fixed wavelength of 4.75 Å. The reflectivity data were analyzed using model functional forms. The SLD profile was approximated by dividing the entire profile into 2 Å thick slabs and varying the SLD according to various functional forms. The number of adjustable parameters was either 4 or 5 depending upon the functional form. The reflectivity was calculated from the stack of slabs using the optical matrix method.[25,26] Best-fit profiles were determined by minimization of least squares.

For the X-ray reflectivity (XR) measurements, a similar protocol was followed except that the solutions were prepared in pure $H_2O$. The XR measurements were performed at the BW1 (undulator) beam line at the HASYLAB synchrotron source (Hamburg, Germany) using a dedicated liquid surface diffractometer.[27] The data were analyzed in a manner analogous to that for NR.[28] The interfaces were smeared using a Gaussian function.

Turbidity experiments were performed using a helium−neon laser (Uniphase, model 1300 series), operating at a wavelength of 633 nm. PSS1150 solutions with varying polymer concentration at KCl concentrations of 0.01, 0.67, and 2.5 M were prepared in rectangular quartz cuvettes. The turbidity of the solutions was obtained from the ratio of the transmitted intensity to the incident intensity.

A series of surface tension measurements were performed following the reflectivity work using the Wilhelmy plate method with a sandblasted platinum plate and a Q11 force transducer from Hottinger-Baldwin. The plate was flamed prior to each series of measurements to remove adsorbed organic material. A few measurements were also performed using a filter paper. No difference was observed in the results of the two methods. The time dependence was examined by comparing measurements performed within a few minutes of creating the interface to those after 4 h for solutions of PSS1150 at 0.01 g/mL and KCl concentrations of 1.7 and 2.5 M. No variation in surface tension was detected over this time period.

## Results

NR data for solutions of d-PSS1150 at 0.67 and 2.50 M KCl are shown in Figure 1a and Figure 2a, respec-

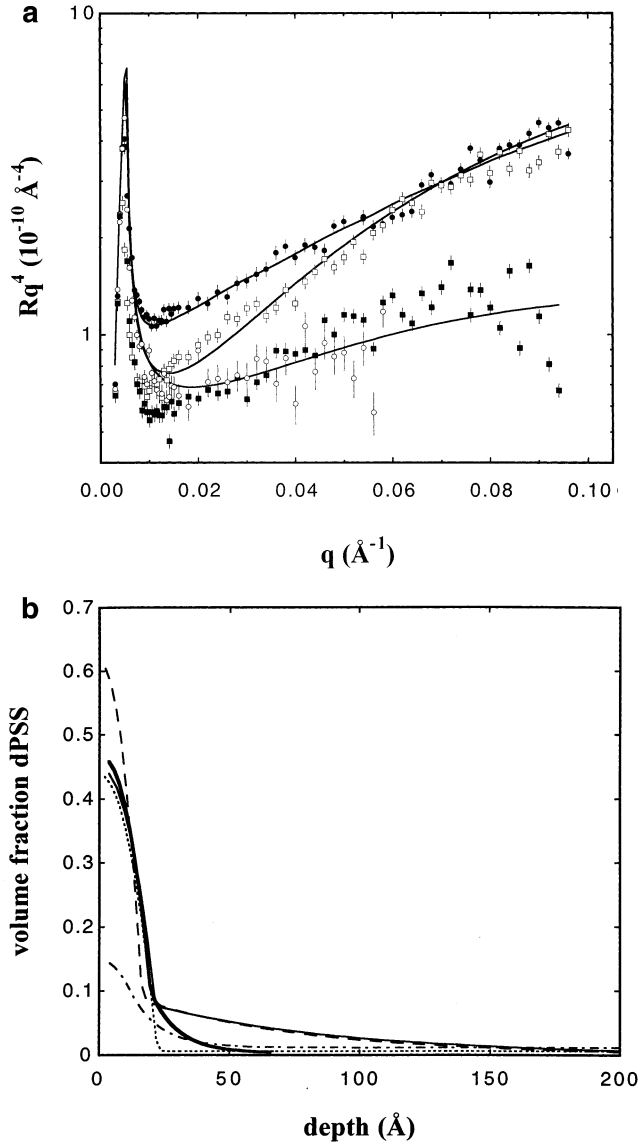


**Figure 1.** (a) Neutron reflectivity data from PSS1150 solutions at 0.67 M KCl: subphase (○), 0.0001 g/mL (●), 0.005 g/mL (□), and 0.01 g/mL PSS (■). The curves through the data correspond to best fits using functional form model profiles. (b) Best-fit segment concentration profiles corresponding to 0.0001 (—), 0.001 (- - -), 0.003 (—), 0.005 (· · ·), and 0.01 g/mL PSS (— · —).

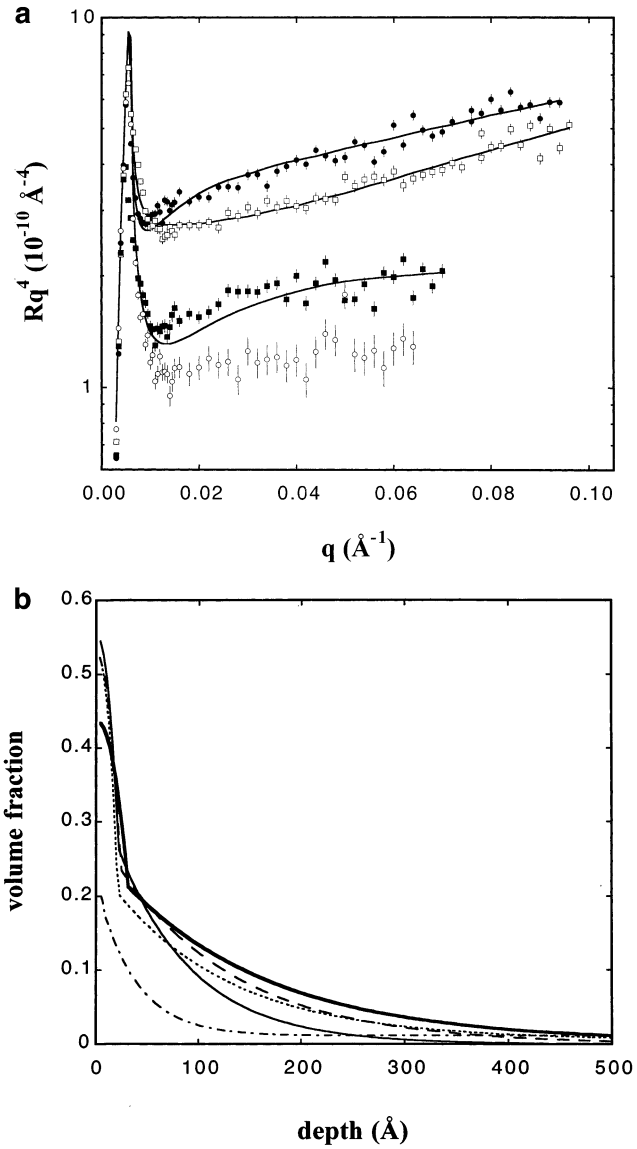


**Figure 2.** (a) Neutron reflectivity data from PSS1150 solutions at 2.50 M KCl: subphase (○), 0.0001 (●), 0.005 (□), and 0.01 g/mL PSS (■). The curves through the data correspond to best fits using functional form model profiles. (b) Best-fit segment concentration profiles corresponding to 0.0001 (—), 0.001 (- - -), 0.003 (—), 0.005 (· · ·), and 0.01 g/mL PSS (— · —).

tively, for several PSS concentrations. The data are displayed as reflectivity × $q^4$ to compensate for the $q^{-4}$ decay due to the Fresnel law and thus more clearly reveal differences in the curves. For both KCl concentrations, the reflectivity initially increases with PSS concentration, reaches a maximum at very low PSS concentration, and then decreases strongly with further increase in PSS concentration. At a PSS concentration of 0.01 g/mL, the reflectivity at 0.67 M KCl is nearly identical to that for the pure $H_2O/D_2O$ subphase. For 2.50 M KCl, the reflectivity at 0.01 g/mL is only slightly higher than that of the pure $H_2O/D_2O$ subphase.

Best-fit segment concentration profiles are shown in Figures 1b and 2b. Segment concentrations were calculated from the SLD values assuming a uniform distribution of $K^+$ and $Cl^-$ ions and $Na^+$ condensation on the d-PSS chains. The values are not significantly different if $Na^+$ is replaced by $K^+$ in the calculation. The calculated SLD of a pure melt of d-$PSS^-Na^+$ is 3.1 × $10^{-6}$/Å$^2$, assuming a mass density of 0.83 g/cm$^3$. At low polymer concentration, the profiles are composed of a thin layer of high concentration at the air surface (trains), followed by a distinct second layer of much lower segment concentration that extends to much larger depths into the liquid (loops and tails). This was discussed in our previous report.[23] The thickness of the first layer is 20 ± 10 Å. A bilayer profile is not required at the highest polymer concentrations, but rather a smoothly decaying one-layer profile is adequate. However, since the signal becomes weak at high PSS concentration, there is substantial uncertainty in the profile shape determined in the fitting for that case.

Figure 3a and Figure 4a show reflectivity data for d-PSS56 at several polymer concentrations for 0.67 and 2.50 M KCl, respectively. For d-PSS56 with 0.67 M KCl, the reflectivity decreases strongly with increasing polymer concentration above 0.005 g/mL. The reflectivity for PSS56 with 2.50 M KCl increases with increasing

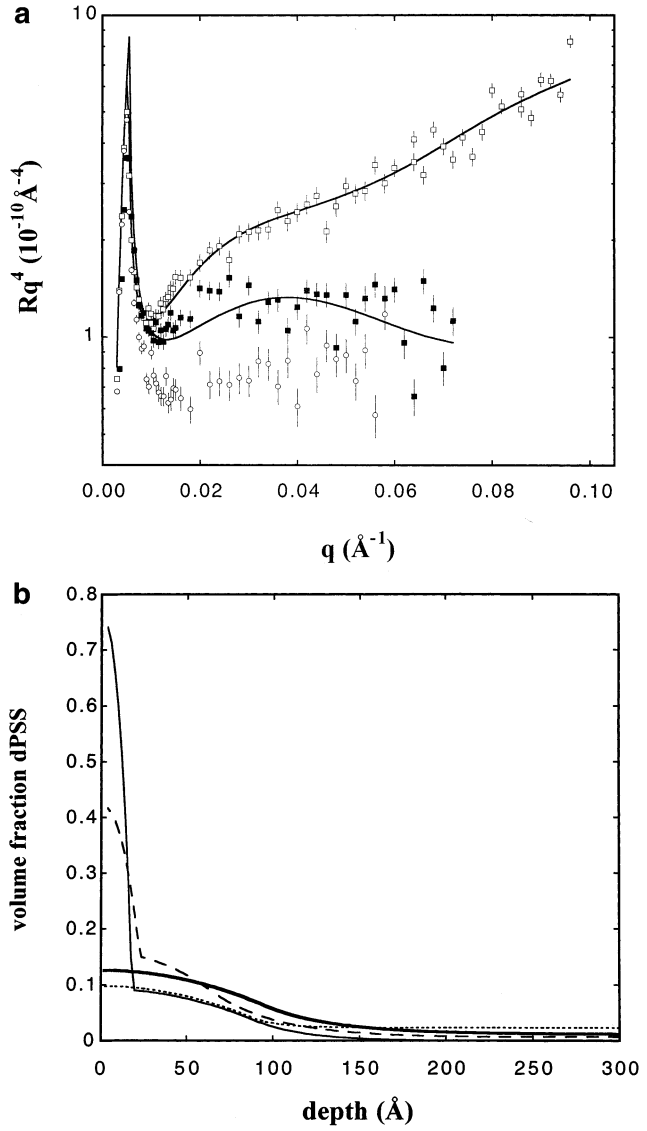


**Figure 3.** (a) Neutron reflectivity data from PSS56 solutions at 0.67 M KCl: subphase (○), 0.001 (□), and 0.02 g/mL PSS (■). The curves through the data correspond to best fits using functional form model profiles. (b) Best-fit segment concentration profiles corresponding to 0.001 (—), 0.005 (- - -), 0.01 (—), and 0.02 g/mL PSS (• • •).

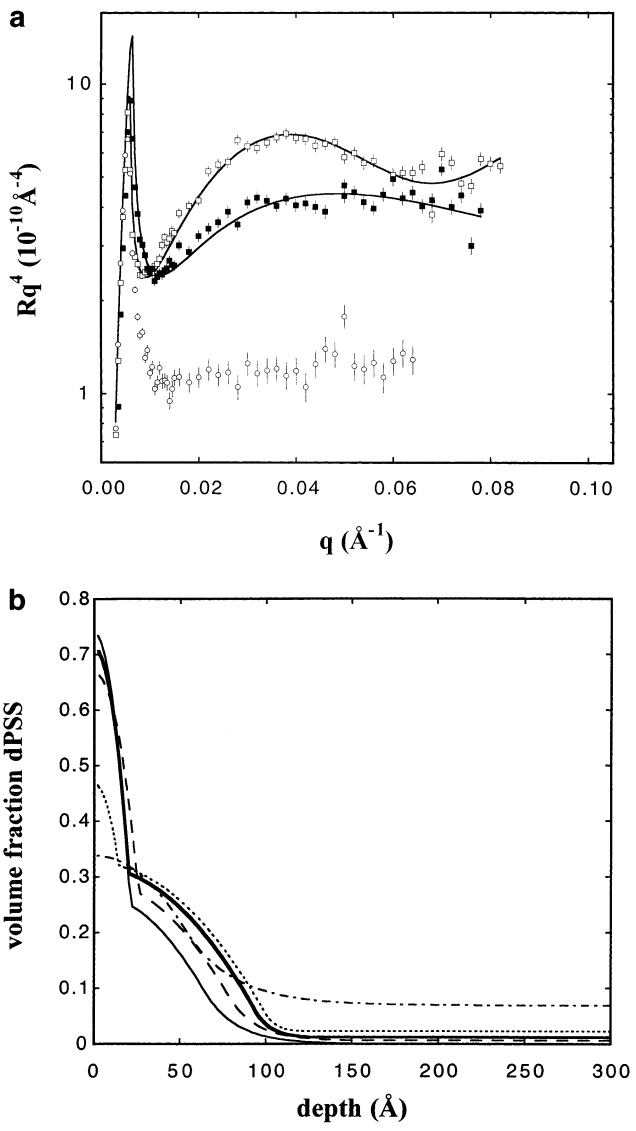


**Figure 4.** (a) Neutron reflectivity data from PSS56 solutions at 2.50 M KCl: subphase (○), 0.01 (□), and 0.067 g/mL PSS (■). The curves through the data correspond to best fits using functional form model profiles. (b) Best-fit segment concentration profiles corresponding to 0.001 (—), 0.005 (- - -), 0.01 (—), 0.02 (• • •), and 0.067 g/mL PSS (— • —).

polymer concentration until roughly 0.01 g/mL, beyond which a strong decrease is again observed. Best-fit segment concentration profiles are shown in Figures 3b and 4b. For d-PSS56 at low polymer concentration, a distinct second layer is again required, although the functional form for the extended layer is different from that for the d-PSS1150 sample. The data are consistent with a functional form consisting of the sum of two parabolas combined with an exponential tail. A smoothly decaying single-layer profile is again consistent with the data at higher polymer concentration.

For both samples, the dependence of adsorbed amount on polymer concentration is plotted for 0.67 and 2.5 M KCl in Figure 5 and Figure 6, respectively. The surface excess is given by $\rho\int(\phi(z) - \phi_b)\,d(z)$, where $\rho$ is the density of d-PSS and $\phi(z)$ is the volume fraction of chain segments near the surface. The absolute adsorbed amount is given by $\rho\int\phi(z)\,d(z)$, integrated to the depth at which the bulk concentration is obtained. The dependence of adsorbed amount on the molecular weight is much stronger at the higher salt concentration (2.50 M). We note that the adsorbed amount for both samples initially increases with polymer concentration, reaches a maximum, and then decreases above a certain polymer concentration. For both molecular weights the maximum shifts to higher PSS concentration when the salt concentration increases from 0.67 to 2.50 M. For both salt concentrations, the maximum in adsorbed amount occurs at higher polymer concentration for d-PSS56 than for d-PSS1150.

X-ray reflectivity was also obtained for certain solution conditions. XR is much more sensitive to the distribution of salt and counterions at the air surface than NR, but is much less sensitive to the PSS segment concentration. Figures 7a and 8a show X-ray reflectivity data for solutions of d-PSS1150 at 0.001 and 0.01 g/mL d-PSS, respectively, with 0.67 M KCl. Curves are also shown for a subphase of 0.67 M KCl without PSS. The data are displayed as the reflectivity divided by the Fresnel reflectivity $R_F$ for an infinitely sharp interface. This ratio can be expressed as[25]

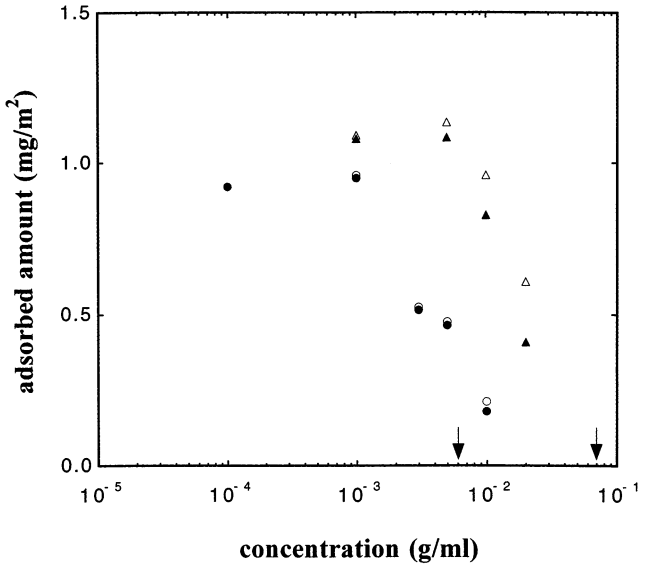


**Figure 5.** Surface excess (filled symbols) and absolute adsorbed amount (open symbols) at the air surface of the aqueous subphase with 0.67 M KCl as a function of polymer concentration for PSS1150 (●) and PSS56 (▲).

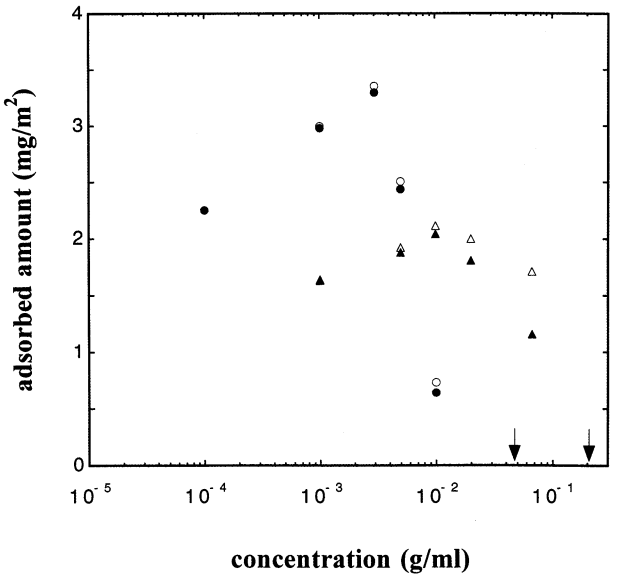


**Figure 6.** Surface excess (filled symbols) and absolute adsorbed amount (open symbols) at the air surface of the aqueous subphase with 2.50 KCl as a function of polymer concentration for PSS1150 (●) and PSS56 (▲).

$$\frac{R}{R_F} = |\frac{1}{\rho_{sub}}\int \rho'(z)e^{iq_z z}\,dz|^2 \qquad (1)$$

where $\rho_{sub}$ is the electron density of the bulk phase, $\rho'(z)$ is the gradient of the electron density along the surface normal, and $q_z$ is the wave vector normal to surface. For pure water $\rho_{sub} = 0.334$ e$^-$/Å$^3$, and at 0.67 M KCl $\rho_{sub} = 0.340$ e$^-$/Å$^3$. The data for the solution of 0.67 M KCl in water are well described by a uniform subphase with 2.8 Å roughness at the air surface. The difference in the data for the solutions with PSS relative to that in absence of PSS indicates the magnitude of the signal and the structure in the curve that arises from nonuniform ion distributions upon adsorption of PSS. With PSS present in solution, the data show a maximum in reflectivity at roughly $q = 0.15$ Å$^{-1}$ and a stronger decrease in reflectivity with $q$ for $q > 0.20$ Å$^{-1}$. Most notably, at low PSS concentration (0.001 g/mL), the X-ray reflectivity contains a distinct minimum at $q = 0.6$ Å$^{-1}$, which indicates that a well-defined layer with elevated electron density exists within the interfacial region. The minimum in the reflectivity data at $q = 0.6$ Å$^{-1}$ observed for the lower polymer concentration is not present at higher polymer concentration (0.01 g/mL), as shown in Figure 8a. The maximum at $q = 0.15$ Å$^{-1}$ is also weaker at the higher PSS concentration. The curves through the data correspond to the electron density profiles shown in Figures 7b and 8b. All electron density profiles are normalized by the electron density of the subphase. The best-fit electron density profile shown in Figure 7b contains a ~10 Å layer with electron density of 0.405 e$^-$/Å$^3$. Importantly, the maximum in electron density is displaced from the surface by ~10 Å. The best-fit profile shown in Figure 8b indicates that

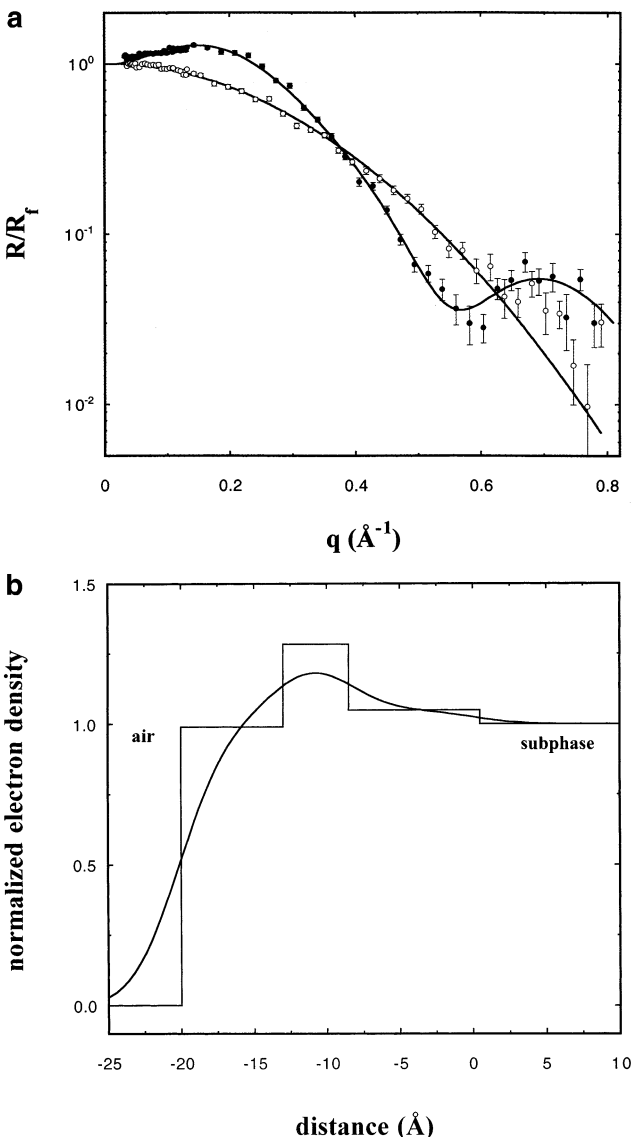


**Figure 7.** (a) X-ray reflectivity data for PSS1150 at 0.001 g/mL with 0.67 M KCl (●). The curve through the data corresponds to the best fit using a model profile consisting of several boxes and variable interfacial roughness. Also shown is the reflectivity in the absence of PSS1150 (○). The curve through these data corresponds to a uniform subphase with 2.8 Å roughness at the air surface. (b) Normalized electron density profile corresponding to the curve through the data with PSS1150 in (a). The layers are also shown without smearing.

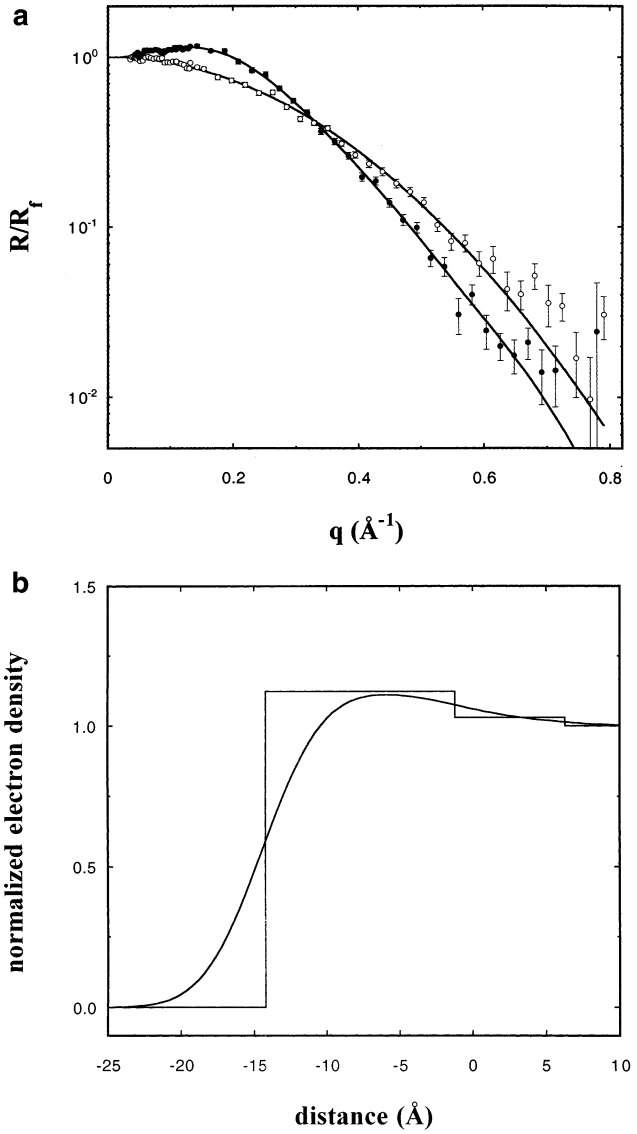


**Figure 8.** (a) X-ray reflectivity data for PSS1150 at 0.01 g/mL with 0.67 M of KCl (●). The curve through the data corresponds to best-fit box model profile shown in (b). The data are again compared with the data in the absence of PSS1150 (○). (b) Normalized electron density profile corresponding to the curve through the data with PSS1150 in (a).

the thin layer of high electron density becomes much weaker and broader at the higher PSS concentration. The dissipation of the peak in electron density occurs over roughly the same range of d-PSS concentration as the decrease in the adsorbed amount observed by NR. Similar thin layers of elevated electron density have been reported for the PSS blocks of PSS−PEE amphiphillic diblock copolymers at the air−water interface by Ahrens et al.,[29,30] although their data extended only to $q = 0.5$ Å so the minimum in reflectivity corresponding to the layer was not directly observed. Finally, we note that reflectivity for a solution of PSS1150 at 0.001 g/mL in water with no added salt (not shown) was nearly indistinguishable from that for the subphase in absence of PSS, which likely indicates that the surface concentration of PSS was too dilute to be detected.

The surface tension of PSS1150 solutions with varying PSS concentration is plotted as a function of KCl concentration in Figure 9. First, this plot shows that the surface tension of a pure KCl solution increases with KCl concentration. This effect is well-known.[31,32] The

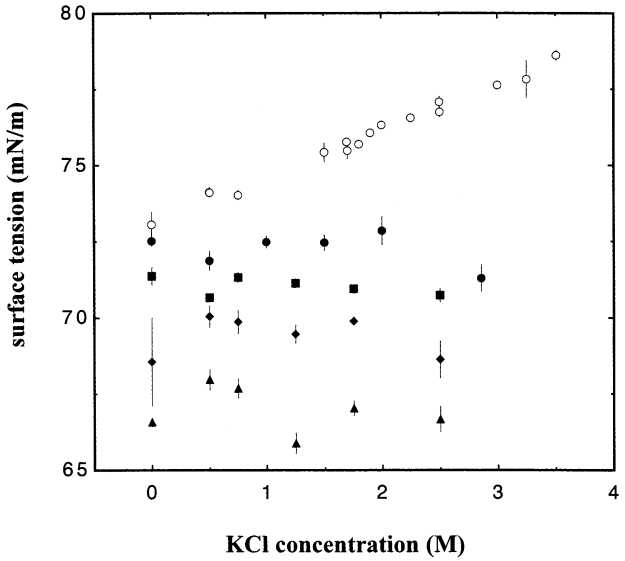


**Figure 9.** Surface tension of PSS1150 solutions as a function of salt (KCl) concentration with varying polymer concentration: subphase (○), 0.001 (●), 0.003 (■), 0.005 (◆), and 0.01 g/mL PSS (▲).

increase in surface tension results from the depletion of ions near the surface due to image charge repulsion and ion hydration. The surface tension of electrolytes at low concentration was first explained by Onsager and Samara.[33] At high electrolyte concentrations the surface tension has been accurately calculated using the modified Poisson−Boltzmann approximation[34] or in the canonical ensemble.[35] Second, this plot shows that for any particular polymer concentration the surface tension is nearly constant with increasing salt concentration, despite the fact that dramatic changes occur in the adsorbed PSS segment profile. Third, there is a steady decrease in surface tension with increasing polymer concentration. The latter observation was reported for PSS solutions in the absence of salt by Caminati and Gabrielli.[21]

## Discussion

**Adsorbed Layer Structure for Low d-PSS Concentration.** We begin by discussing the surface structure that occurs for dilute d-PSS concentration. The peak in the electron density determined from X-ray reflectivity can only be interpreted as an elevated concentration of $Na^+$, $K^+$, or $Cl^-$ ions, as the electron density of PSS is lower than that of water.[36] We emphasize that the peak in electron density is not immediately at the surface, but at a depth of about 10 Å below the surface. This corresponds well to the dimension of a PSS monomer.[37] This suggests a surface structure in which the PSS segments lie at the surface with the low-energy backbone exposed to the air while the sulfonate groups are submerged into the liquid, as illustrated schematically in Figure 10. An analogous structure was seen in simulations of a monolayer of sodium dodecyl sulfate (SDS) at the air−water interface.[38] The dense layer of ions revealed in the data of Figure 7 likely consists of counterions closely bound to adsorbed PSS segments. To calculate the theoretical electron density for a layer composed of $K^+SO_3^-$, a knowledge of the density of $K^+SO_3^-$ within the layer is required. For an estimate in the limit of strong association, we use the density of potassium dithionate ($K_2S_2O_6$), 2.278 g/cm$^3$. The calculated electron density is then

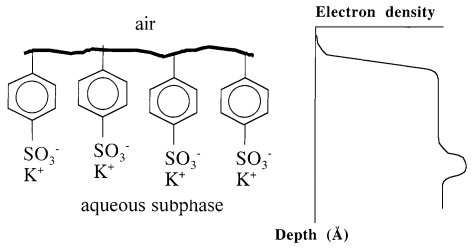


**Figure 10.** Schematic diagram of PSS chain segments with counterions at the air/water interface. The condensed ions correspond to a high electron density layer. This profile is convoluted with the roughness in the experimental profile.

0.682. Such a layer would more than account for the measured peak electron density of the thin layer of 0.403 $e^-/Å^3$. It is unlikely that the density of $K^+SO_3^-$ in the near-surface layer is as high as in solid potassium dithionate. The measured electron density of 0.403 $e^-/Å^3$ corresponds to a density of 1.35 g/cm$^3$ in the layer, assuming only $K^+SO_3^-$ (no water molecules).

A strong association of $K^+$ and $SO_3^-$ near the air surface can be explained by the enhanced Coulomb interaction that occurs in the near surface region. The air−water interface possesses a discontinuity in the dielectric constant. The effect on the electrostatic interactions between ions in the solution can be calculated by the image charge method.[39] The image charge method is one means to include the proper boundary conditions at a dielectric discontinuity. Let the dielectric constants be $\epsilon_a$ in air and $\epsilon_w$ in water. The electric potential at point P described by cylindrical coordinates $(r,\phi,z)$ due to a charge Q in solution a distance $d$ from the interface is the sum of the potentials due to charge Q and its image charge Q′,

$$\Phi = \frac{1}{\epsilon_w}\left(\frac{Q}{R_1} + \frac{Q'}{R_2}\right) \tag{2}$$

where $R_1 = [r^2 + (d - z)]^{1/2}$, $R_2 = [r^2 + (d + z)]^{1/2}$, and $Q' = Q(\epsilon_w - \epsilon_a)/(\epsilon_w + \epsilon_a)$. One effect of the image charge is the repulsion of any ion from the interface. Taking $\epsilon_w$ to be 78 and $\epsilon_a$ to be 1, $Q' = 77/79Q$. If we consider the case where the point P is also at the distance $z = d$ from the interface, then

$$\Phi = \frac{Q}{\epsilon_w r}\left(1 + \frac{R_1}{R_2}\frac{77}{79}\right) \cong 2\Phi_w \tag{3}$$

where $\Phi_w$ is the bulk potental in water, i.e., $Q/\epsilon_w r$. Thus, the interactions are altered such that the dielectric constant at the interface is one-half that of the bulk. This makes the attractive Coulomb interactions between oppositely charged ions stronger. In other words, the Bjerrum length is doubled at the interface. Thus, for a pair of oppositely charged ions in the interfacial region, their attraction will be about twice as strong as in the bulk, but they will be repelled from the interface by their image charges.[34]

For polyelectrolyte chains, the increased Coulomb interaction near the interface likely has a significant effect on the structure of the adsorbed layer. The amount of counterion condensation depends on the value of the Bjerrum length. The larger value at the interface increases the amount of counterion condensation. Even though counterions are repelled from the surface, they are more strongly attracted to the oppositely charged sulfate groups just below the surface

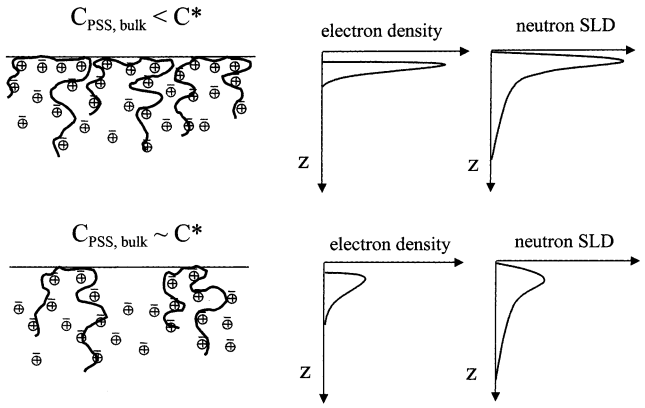


**Figure 11.** Schematic diagram of PSS chain segments with ions at the air/water interface for two different polymer concentrations.

than in the bulk. We note that no excess of election density was observed in the absence of d-PSS. This is expected due to the repulsion of ions from the surface.[34] Thus, the layer of excess electron density is clearly associated with the adsorption of polymer segments. We note further that the layer of localized ions, while observed for a PSS solution with 0.67 M KCl, was not observed in the absence of salt. In the absence of salt the adsorbed chains are likely too dilute to be detected. Salt is required to allow the chains to pack densely at the surface and produce a measurable signal.

This result from X-ray reflectivity helps to explain the bilayer profiles obtained from the NR data. The distinct bilayer profiles contrast with the smoothly varying single-layer profile predicted by SCF theory.[4] This theory did not specifically treat the air surface and so did not include the effect of the enhanced Coulomb interaction, the depletion of salt from the surface, or the strong attraction of the low-energy backbone to the surface. These effects result in a thin layer of elevated SLD near the air surface. In the NR profiles, the thin layer at the air surface has a dimension of 20 ± 10 Å. This thickness includes the dense layer of ions as well as PSS segments.

**Variation in Layer Structure with d-PSS Concentration.** The most surprising result in our study is that the adsorbed amount for both molecular weights reaches a maximum and then decreases with polymer concentration in the semidilute regime, as shown in Figures 5 and 6. Both NR and XR data show that the thin layer at the air surface dissipates with increasing polymer concentration. The results are summarized in the illustration in Figure 11. The fact that the adsorbed amount decreases, rather than simply remaining constant, with increasing d-PSS concentration is particularly striking. The adsorption of polymer segments to the air surface is driven by a decrease in surface energy, which can be estimated as $a^2S$, where $a^2$ is the area per monomer and $S = \gamma_{air/water} - \gamma_{air/PSS} - \gamma_{PSS/water}$, where $\gamma_{air/water}$, $\gamma_{air/PSS}$, and $\gamma_{PSS/water}$ are the interfacial tensions. Assuming that the low surface energy backbone of PSS has the same surface energy as polystyrene (40 mN/m), that the interfacial tension between PSS and water is negligible, and an area per monomer of 36 Å$^2$, then the adsorption energy per monomer is $2.8kT$. Since the backbone of PSS is hydrophobic, the interfacial tension between PSS and water is likely to be significant. Therefore, the value of $2.8kT$ per monomer is an upper limit. The observed decrease in the segment concentra-

tion at the surface with increasing PSS concentration implies that there must be effects which compensate for an increase in surface free energy of this magnitude.

Furthermore, the fact that the transition is a function of molecular weight and salt concentration suggests a relationship with the overlap polymer concentration, $C_p^*$. The polymer overlap concentration, which is the demarcation between the dilute and semidilute concentration regimes, may be defined analogous to that for uncharged macromolecules with the following equation:[40]

$$C_p^* = N/R_G^3 \sim N^{1-3\nu} \quad (4)$$

where $N$ is the degree of polymerization and $R_G$ is the radius of gyration of the polyelectrolyte. A value for $R_G$ of 140 Å has been reported for d-PSS with a molecular weight of 72 000 g/mol (including $Na^+$ counterions) in pure water.[8] The molecular weight of d-PSS56 is 62 000 g/mol (including $Na^+$ counterions). With no added salt, the solvent quality of PSS in water is better than that for PS in a good solvent such as toluene, and the relationship $R_G \sim N^{0.82}$ was determined by MD simulations.[17] Using this relationship and the data for $R_g$ of the 72 000 g/mol sample, we estimate $R_G$ of d-PSS56 in pure water to be ~124 Å. Guenoun et al. measured $R_G$ as a function of salt concentration for NaPSS/PtBS diblock copolymers with very short PtBS blocks.[41] They found that $R_G$ of NaPSS/PtBS (83 000/4200 g/mol) in pure water decreases by a factor of 0.57 with addition of salt (NaCl) to 0.5 M. Using this factor and the above estimate of $R_G$ of d-PSS56 in pure water, we estimate that $R_G$ of d-PSS56 in 0.67 M KCl solution to be ~71 Å. This gives a value of $C_p^*$ of 0.069 g/cm$^3$. To estimate $C_p^*$ for d-PSS1150, the molecular weight scaling relationship at 0.67 M KCl is required. Elsewhere, it was shown that $D \sim M^{-0.6}$ for PSS in 0.15 M NaCl,[42] where $D$ is the diffusion coefficient. Using $\nu = 0.6$ in eq 4, we estimate $C_p^*$ to be 0.0061 g/cm$^3$ for d-PSS1150 with 0.67 M KCl. For 2.50 M KCl, the bulk chain conformations should be close to Gaussian as the Θ solvent condition is known to occur at a KCl concentration of 3.1 M.[42,43] $R_G$ for d-PSS with a molecular weight of 72 000 g/mol at the Θ condition has been reported to be 52 Å.[8] With $\nu = 0.5$ for a Gaussian chain in eq 4, the $C_p^*$ values for d-PSS56 and d-PSS1150 at 2.50 M KCl are estimated as 0.21 and 0.047 g/cm$^3$, respectively. Note that the transition points in Figures 5 and 6 occur consistently at concentrations about an order of magnitude lower than the estimated chain overlap concentrations (shown as arrows).

Thus, we consider effects that would lead to a lower free energy for free chains in solution relative to chains adsorbed at the surface, and that depend on molecular weight and salt concentration in a manner consistent with that of the chain overlap concentration. A particular challenge is to explain how the bulk polyelectrolyte concentration can affect the layer structure even in the presence of high salt concentration, where Coulomb interactions should already be strongly screened. Below we offer two possibilities along with counter arguments.

First, we consider the depletion of salt near the surface and the possibility of interchain screening of the Coulomb interactions in that region. This could explain a polymer concentration effect in the presence of high bulk salt concentration. The argument focuses on a competition between chain configurational entropy and image charge repulsion which favor loops and tails over trains, and the segmental adsorption energy which drives adsorption. Image charge repulsion will increase the free energy of segments near the surface relative to segments in the bulk. The magnitude of this effect will be given by $kT \times$ (Bjerrum length divided by the distance of the ions from the surface), which will also be of order $kT$/(monomer in the near surface region). We expect this effect to be largely independent of PSS concentration. Thus, in this view the dependence on overlap concentration must arise due to interchain screening. Interchain screening in the near surface region where salt is depleted would result in a decreasing persistence length for the chains until the intrinsic, neutral value is reached. With Coulomb interactions highly screened, chain entropy dominates favoring loops and tails over trains. This effect alone is unlikely to account for the desorption of chains from the surface as overlap is reached,[44] but in combination with image charge repulsion would lead to fewer adsorbed segments per chain. However, arguing against this explanation is the fact that an elevated concentration of PSS segments in the salt-depleted region is required for screening, yet this region is very small and appears to coincide with the first layer of the bilayer profiles, for which we observe a strong *decrease* in adsorbed segment density with bulk PSS concentration.

Alternatively, the transition may be related to the appearance of associations or aggregates in solution. Evidence for interchain aggregation or association in aqueous solutions of PSS has been reported previously,[10−13] apparently indicating that an attractive interaction occurs among the PSS chains in the bulk. Several researchers have reported the existence of two relaxation modes in polyelectrolyte solutions containing monovalent salt by dynamic light scattering.[10−13] The fast relaxation mode is interpreted as a cooperative diffusion of polyions and counterions. It seems that the existence of polyelectrolyte aggregates or domains can give a satisfactory interpretation for the slow mode. There have been conflicting reports regarding the solution conditions for the appearance of double-exponential correlation functions. One group reported a single-exponential decay at high salt concentrations, but the correlation functions became double exponential as the concentration of added salt was reduced.[10] On the other hand, Sehgal and Seery[12] reported double-exponential correlation functions over a wide range of salt concentrations for PSS in *N*-methylformamide, and Sedlak[45] reported for NaPSS in aqueous NaCl solutions that the slow mode can persist until Θ conditions (4.17 M NaCl) at sufficiently high polymer concentration. Recently, Tanahatoe and Kuil[13a] studied the diffusion coefficient of NaPSS for molecular weights ranging from 77 to 350 kg/mol over PSS concentrations ranging from 1 to 40 g/L at a fixed NaCl concentration of 0.01 M. They found that at the lowest polymer concentration the correlation functions were single-exponential. As the polymer concentration increased beyond 0.001 g/mL, double-exponential correlation functions were obtained. The polymer concentration at which the slow diffusion coefficient started to appear roughly matched $C_p^*$. In addition to studying the autocorrelation functions, they were able to directly image aggregates in solution by optical microscopy. They also reported an increase in total scattered intensity with increasing PSS concentration beginning at about 0.001 g/mL. In further work, they

reported that for a 77 kg/mol PSS sample the size of the aggregated domains decreased with increasing ionic strength.[13b] They reported that the aggregates were not an artifact of their purification procedures, as double-exponential correlation functions were obtained for solutions made from as-received materials without further dialyzing the polymer or filtering as well as from solutions made after dialyzation and filtration (0.65 $\mu$m pore size).

Considering the presence of aggregates in the bulk, we performed turbidity measurements as a function of PSS and KCl concentration for PSS1150. Whereas the solutions all appeared clear to the eye, a significant decrease in transmitted intensity was measured with increasing PSS concentration beginning at $C_{PSS} = 0.001$ g/mL. The PSS concentration where the transmitted intensity began to decrease was nearly independent of salt concentration from 0.01 to 2.5 M KCl, but we cannot rule out a weak dependence. Our turbidity measurements are qualitatively consistent with the measurements of total scattered intensity at 90° reported by Tanahoe and Kuil.

Thus, there is evidence that PSS chains associate in aqueous solutions containing monovalent salts far from any phase boundary. (We reiterate that the Θ condition for the present system has been estimated at 3.5 M KCl, which is greater than the concentration used in the present work.) The reason for an interchain association in these solutions has been puzzling.[46−50] Nevertheless, the present data on the adsorbed layer structure at the air surface may provide independent support for the notion of an association between chains within the bulk solution, suggesting that the decrease in free energy upon association is sufficient to overcome the adsorption energy. The question then arises as to why the aggregates of associated chains do not adsorb at the air surface. One possibility is that the hydrophobic backbones of the d-PSS chains associate in a way that leaves the charged groups exposed at the periphery of the aggregates. In that case, the aggregates would be repelled from the surface. Another possibility is that the aggregates do indeed adsorb but with a very dilute segment density.

We note that two groups previously used neutron scattering to study the small scale structure of bulk aqueous solutions of PSS over a similar salt and PSS concentration range as in the present work. Spiteri et al. measured the persistence length of NaPSS in solutions of NaBr for two polymer concentrations as a function of salt.[9] They examined only the form factor and reported no data for the structure factor. Their results indicate that the persistence length depends on only $c_{pss} + 2c_{salt}$, which led them to question counterion condensation at the nanometer level. Another recent study examined the total scattering from semidilute solutions of NaPSS in the presence of barium chloride.[51] With increasing divalent salt concentration, the scattering at low $q$ diverged smoothly as the phase boundary was approached. Neither of these studies reported evidence of anomalous aggregation away from a phase boundary, which may indicate that the interchain association does not strongly affect the small scale structure of the chains.

**Surface Tension.** Finally, we turn to the surface tension data. Interestingly, we find that the surface tension varies monotonically with the concentration of PSS in bulk solution but does not correlate with the concentration of PSS at the surface. In Figure 9 for all salt concentrations examined, there is a continuous decrease in surface tension with increasing d-PSS concentration in solution. However, for fixed d-PSS concentration in solution, little or no change in surface tension is observed as a function of salt concentration, even though the adsorbed segment profiles of d-PSS vary dramatically. This contrasts sharply with the behavior for solutions of uncharged polymers where polymer adsorption corresponds to a decrease in surface tension.[52,53] Moreover, for uncharged polymers the surface tension has been shown to be independent of the bulk solution concentration over a wide range for the case of a depletion of polymer at the surface.[52,54] Thus, the relationships between the surface tension and the surface and bulk polymer concentrations are very different for charged and uncharged polymers. While a theory for the surface tension of solutions containing uncharged polymers was presented a number of years ago,[52] to our knowledge no such theory has yet been offered for solutions of charged polymers. We do not have an interpretation of these data as yet but simply note that surface tension is not an indicator of adsorbed amount in this strong polyelectrolyte system. A similar finding was reported by Frommer and Miller in their study of the adsorption of DNA at the air surface of aqueous buffer solution.[55] Significant adsorbed amounts were determined using tritium-labeled DNA, and yet little or no change in surface tension was observed. Theodoly et al. arrived at a similar conclusion in their study of the surface tension of aqueous solutions of partially sulfonated PSS.[22] They successively exchanged the solution underneath an adsorbed polymer layer with pure water and a salt solution and found that the surface tension oscillated repeatedly between the same two values. Since the surface tension values were reproducible with repeated exchanges, the authors concluded that the changes in surface tension could not be explained by changes in the adsorbed amount, but rather by electrostatic effects due to changes in the ionic strength of the bulk solution.

The Gibbs adsorption equation can be written as[56]

$$-\frac{d\gamma}{RT} = \Gamma_{PSS} d(\ln c_{PSS} f_{PSS}) + \Gamma_{ci} d(\ln c_{ci} f_{ci}) + \Gamma_{salt} d(\ln c_{salt} f_{salt}) \quad (5)$$

where $\gamma$ is the surface tension, $\Gamma_i$ are surface excesses, $c_i$ are the concentrations, $f_i$ are the activity coefficients, and the subscript "ci" refers to counterion. The experimental finding $d\gamma/d(\ln c_{salt}) = 0$ in Figure 9 leads to the following relationship:

$$\Gamma_{PSS} \left.\frac{\partial(\ln f_{PSS})}{\partial(\ln c_{salt})}\right|_{c_{PSS}} + \Gamma_{ci} \left.\frac{\partial(\ln f_{ci})}{\partial(\ln c_{salt})}\right|_{c_{PSS}} = -\Gamma_{salt}\left(\left.\frac{\partial(\ln f_{salt})}{\partial(\ln c_{salt})}\right|_{c_{PSS}} + 1\right) \quad (6)$$

for the range of salt concentration examined. This relationship indicates that changes in PSS adsorbed amount with varying salt concentration are compensated by changes in the distribution of salt near the surface or by changes in the activity coefficients. We expect that the activity coefficients are sensitive to the size and valency of the counterions. This will be investigated in future work.

## Summary

We have investigated the adsorption of d-PSS to the air surface of aqueous solutions as a function of PSS concentration, molecular weight, and salt concentration. We combine direct measurements of the polymer segment distribution by neutron reflection, the counterion distribution by X-ray reflection, and the surface free energy by surface tension measurements. At low polymer concentration, a bilayer profile is obtained from NR, composed of a thin layer of high scattering length density at the air surface and a distinct second layer of much lower scattering length density that extends well into the subphase. The combination of NR and XR suggests that the near surface region is actually composed of a dense layer of polymer segments at the surface (trains) followed by a dense layer of counterions. With increasing polymer concentration, we find that the dense layer of segments and counterions at the air surface both dissipate, and the profiles tend toward a smoothly decaying one-layer profile. Correspondingly, the adsorbed amount for both molecular weights first increases, reaches a maximum, and then decreases with d-PSS concentration. The decrease in adsorbed amount with polymer concentration is dependent on both the molecular weight and salt concentration in the solution in a way that suggests a dependence on the chain overlap concentration. This transition may be related to reports of interchain associations in the bulk of PSS solutions. Finally, we observe that the surface tension correlates with the concentration of PSS in bulk solution but does not correlate with the amount of PSS adsorbed at the surface.


**Acknowledgment.** This work was supported by the U.S. Department of Energy under Contract CE-AC04-94AL85000. Sandia is a multiprogram laboratory operated by Sandia Corporation, a Lockheed Martin Company, for the United States Department of Energy. We acknowledge the support of the National Institute of Standards and Technology, U.S. Department of Commerce, in providing the neutron facilities used in this work. This work also benefited from the use of the Los Alamos Neutron Science Center at the Los Alamos National Laboratory. This facility is funded by the U.S. Department of Energy under Contract W-7405-ENG-36.

## References and Notes


(1) Napper, D. H. *Polymeric Stabilization of Colloid Dispersions*; Academic Press: New York, 1983.
(2) Dickenson, E. *Curr. Opin. Colloid Interface Sci.* **1998**, *3*, 633.
(3) Fukuzaki, S.; Urano, H.; Nagata, K. *J. Ferment. Bioeng.* **1996**, *81*, 163.
(4) Fleer, G. J.; Cohen-Stuart, M. A.; Scheutjens, J. M. H. M.; Cosgrove, T.; Vincent, B. *Polymers at Interfaces*; Chapman & Hall: London, 1993.
(5) Nierlich, M.; Boue, F.; Lapp, A.; Oberthür, R. *Colloid Polym. Sci.* **1985**, *263*, 955.
(6) Matsuoka, H.; Schwahn, D.; Ise, N. *Macromolecules* **1991**, *24*, 4227.
(7) Seldak, M.; Amis, E. *J. Chem. Phys.* **1992**, *96*, 817.
(8) Boué, F.; Cotton, J. P.; Lapp, A.; Jannink, G. *J. Chem. Phys.* **1994**, *101*, 2562.
(9) Spiteri, M. N.; Boué, F.; Lapp, A.; Cotton, J. P. *Phys. Rev. Lett.* **1996**, *77*, 5218.
(10) Drifford, M.; Dalbiez, J. P. *Biopolymers* **1985**, *24*, 1501.
(11) Reed, W. F. *Macromolecules* **1994**, *27*, 873.
(12) Sehgal, A.; Seery, T. A. P. *Macromolecules* **1998**, *31*, 7340.
(13) Tanahatoe, J. J.; Kuil. M. E. *J. Phys. Chem. B* **1997**, *101*, 9233. Tanahatoe, J. J.; Kuil, M. E. *J. Phys. Chem. B* **1997**, *101*, 10839.
(14) Boris, D. C.; Colby, R. H. *Macromolecules* **1998**, *31*, 5746.
(15) Hirose, E.; Iwamoto, Y.; Norisuye, T. *Macromolecules* **1999**, *32*, 8629.
(16) Takahashi, Y.; Matsumoto, N.; Iio, S.; Kondo, H.; Noda, I.; Imai, M.; Matsushita, Y. *Langmuir* **1999**, *15*, 4120.
(17) Stevens, M. J.; Kremer, K. *J. Chem. Phys.* **1995**, *103*, 1669.
(18) Papenhuijzen, J.; Fleer, G. J.; Bijsterbosch, B. H. *J. Colloid Interface Sci.* **1985**, *104*, 530.
(19) Okubo, T. *J. Colloid Interface Sci.* **1988**, *125*, 386.
(20) Okubo, T.; Kobayashi, K. *J. Colloid Interface Sci.* **1998**, *205*, 433.
(21) Gabrielli, G.; Caminati, G. *Colloids Surf. A* **1993**, *70*, 1.
(22) Theodoly, O.; Ober, R.; Williams, C. E. *Eur. Phys. J. E* **2001**, *5*, 51.
(23) Yim, H.; Kent, M.; Matheson, A.; Ivkov, R.; Satija, S.; Majewski, J.; Smith, G. S. *Macromolecules* **2000**, *33*, 6126.
(24) Vink, H. *Makromol. Chem.* **1981**, *182*, 279.
(25) Russell, T. P. *Mater. Sci. Rep.* **1990**, *5*, 171.
(26) Penfold, J.; Thomas, R. K. *J. Phys.: Condens. Matter* **1990**, *2*, 1369.
(27) Majewski, J.; Popovitz-Biro, R.; Bouwman, W. G.; Kjaer, K.; Als-Nielsen, J.; Lahav, M.; Leiserowitz, L. *Chem.—Eur. J.* **1995**, *1*, 304.
(28) Als-Nielsen, J.; Kjaer, K. X-ray Reflectivity and Diffraction Studies of Liquid Surfaces and Surfactant Monolayers. In *The Proceedings of the NATO Advanced Study Institute, Phase Transitions in Soft Condensed Matter*; *Geilo, Norway, April 4−14, 1989*; Plenum Publishing Corp.: New York, pp 113−137.
(29) Ahrens, H.; Forster, S.; Helm, C. A. *Macromolecules* **1997**, *30*, 8447.
(30) Ahrens, H.; Forster, S.; Helm, C. A. *Phys. Rev. Lett.* **1998**, *81*, 4172.
(31) Weissenborn, P. K.; Pugh, R. J. *J. Colloid Interface Sci.* **1996**, *184*, 550.
(32) Matubayasi, N.; Yamamoto, K.; Yamaguchi, S.-I.; Matuso, H.; Ikeda, N. *J. Colloid Interface Sci.* **1999**, *214*, 101.
(33) Onsager, L.; Samara, N. N. T. *J. Chem. Phys.* **1934**, *2*, 528.
(34) Bhuiyan, L. B.; Bratko, D.; Outhwaite, C. W. *J. Phys. Chem.* **1991**, *95*, 336.
(35) Levin, Y.; Flores-Mena, J. E. *Europhys. Lett.* **2001**, *56*, 187.
(36) Ahrens et al. estimated the electron density of dehydrated PSS to be 0.46 $e^-/Å^3$.[29] We calculate a value of 0.25 $e^-/Å^3$ for PSS. The discrepancy is due to the value of the density (volume per monomer) assumed in the calculation. They assumed that a PSS segment had a volume of 200 $Å^3$. This results in a mass density of 1.53 $g/cm^3$, which is substantially greater than the literature value of 0.801 $g/cm^3$ for h-PSS.[57] We used 0.83 $g/cm^3$ for d-PSS in our calculation.
(37) Donath, E.; Walter, D.; Shilov, V. N.; Knippel, E.; Budde, A.; Lowack, K.; Hjelm, C. A.; Mohwald, H. *Langmuir* **1997**, *13*, 5294.
(38) Dominguez, H.; Berkowitz, M. *J. Phys. Chem. B* **2000**, *104*, 5302.
(39) Jackson, J. D. *Classical Electrodynamics*; Wiley & Sons: New York, 1975.
(40) Hara, M. *Polyelectrolytes: Science and Technology*; Marcel Dekker: New York, 1993.
(41) Guenoun, P.; Davis, H. T.; Tirrell, M.; Mays, J. W. *Macromolecules* **1996**, *29*, 3965.
(42) Wang, L.; Yu, H. *Macromolecules* **1988**, *21*, 3498.
(43) Takahashi, A.; Kata, T.; Nagasawa, M. *J. Phys. Chem.* **1967**, *71*, 2001.
(44) Indeed, poly(ethylene oxide) is a water-soluble flexible chain, yet it adsorbs flat to the surface of water.[58] In that case the decrease in surface free energy upon adsorption is sufficient to overcome the loss in configurational and translational entropy. We would expect that to be the case for PSS as well, as the decrease in surface energy per monomer upon adsorption should be comparable for PEO and PSS in water.
(45) Seldak, M. *J. Chem. Phys.* **1996**, *105*, 10123.
(46) Ise, N. *Angew. Chem., Int. Ed. Engl.* **1986**, *25*, 323.
(47) Wissenburg, P.; Odijk, T.; Cirkel, P.; Mandel, M. *Macromolecules* **1994**, *27*, 306.
(48) Wissenburg, P.; Odijk, T.; Cirkel, P.; Mandel, M. *Macromolecules* **1995**, *28*, 2315.
(49) Schmidz, K. S.; Lu, M.; Gauntt, J. *J. Chem. Phys.* **1983**, *78*, 5059.

(50) Muthukumar, M. *J. Chem. Phys.* **1996**, *105*, 5183.
(51) Prabhu, V. M.; Muthukumar, M.; Wignall, G. D.; Melnichenko, Y. B. *Polymer* **2001**, *42*, 8935.
(52) Ober, R.; Paz, L.; Taupin, C.; Pincus, P.; Boileau, S. *Macromolecules* **1983**, *16*, 50.
(53) Guiselin, O.; Lee, L. T.; Farnoux, B.; Lapp, A. *J. Chem. Phys.* **1991**, *95*, 4632.
(54) Lee, L. T.; Guiselin, O.; Lapp, A.; Farnoux, B.; Penfold, *J. Phys. Rev. Lett.* **1991**, *67*, 2838.
(55) Frommer, M. A.; Miller, I. R. *J. Phys. Chem.* **1968**, *72*, 2862.
(56) Adamson, A. W.; Gast, A. P. *Physical Chemisty of Surfaces*; John Wiley & Sons: New York, 1997.
(57) *Aldrich Catalog and Handbook of Fine Chemicals*; Aldrich: Milwaukee, WI, 1998−1999; p 1391.
(58) Kawaguchi, M.; Sauer, B. B.; Yu, H. *Macromolecules* **1989**, *22*, 1735.

MA0200468